Assessing The Accuracy Of New Geminal-Based Approaches

ARTICLE *in* THE JOURNAL OF PHYSICAL CHEMISTRY A · APRIL 2014

Impact Factor: 2.69

7 AUTHORS, INCLUDING:

Paweł Tecmer

Nicolaus Copernicus University

19 PUBLICATIONS **193** CITATIONS

SEE PROFILE

Katharina Boguslawski

Nicolaus Copernicus University

22 PUBLICATIONS **229** CITATIONS

SEE PROFILE

Paul A. Johnson

McMaster University

15 PUBLICATIONS **202** CITATIONS

SEE PROFILE

Toon Verstraelen

Ghent University

58 PUBLICATIONS **609** CITATIONS

SEE PROFILE

THE JOURNAL OF PHYSICAL CHEMISTRY A

Article

pubs.acs.org/JPCA

Assessing the Accuracy of New Geminal-Based Approaches

Paweł Tecmer,[†] Katharina Boguslawski,[†] Paul A. Johnson,[†] Peter A. Limacher,[†] Matthew Chan,[†] Toon Verstraelen,[‡] and Paul W. Ayers*[,†]

[†]Department of Chemistry and Chemical Biology, McMaster University, 1280 Main Street West, L8S 4M1, Hamilton, Ontario, Canada

[‡]Center for Molecular Modeling, QCMM Alliance Ghent-Brussels, Ghent University, Technologiepark 903, Zwijnaarde 9052, Belgium

Supporting Information

ABSTRACT: We present a systematic theoretical study on the dissociation of diatomic molecules and their spectroscopic constants using our recently presented geminal-based wave function ansätze. Specifically, the performance of the antisymmetric product of rank two geminals (APr2G), the antisymmetric product of 1-reference-orbital geminals (AP1roG) and its orbital-optimized variant (OO-AP1roG) are assessed against standard quantum chemistry methods. Our study indicates that these new geminal-based approaches provide a cheap, robust, and accurate alternative for the description of bond-breaking processes in closed-shell systems requiring only mean-field-like computational cost. In particular, the spectroscopic constants obtained from OO-AP1roG are in very good agreement with reference theoretical and experimental data.

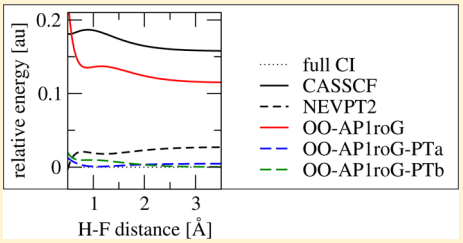

INTRODUCTION

Present-day quantum chemistry seeks simple, robust, and efficient algorithms for a qualitatively correct description of strongly correlated many-body problems. The difficulty in accurately modeling strongly correlated systems emerges from the fact that molecular orbitals become quasi-degenerate.[1−3] In such cases, the orbital model is qualitatively incorrect and the electronic wave function is no longer well-represented by a single Slater determinant. Instead, a qualitatively accurate description of electronic structures requires several Slater determinants, and the system is said to possess strong multireference character.[1−6] Strong electron correlation becomes important in single- and multiple-bond-breaking processes.[7−10] The electronic properties of transition-metal,[11,12] lanthanide,[13] and actinide compounds[14,15] also show the effects of strong electron correlations.

Standard, well-established multireference methods are, for instance, multireference configuration interaction,[16] complete active-space self-consistent field theory,[17,18] restricted active-space self-consistent field theory,[19] and the density matrix renormalization group.[20−24] Different techniques to model the strong electron correlation problem also emerged within multireference coupled-cluster theory,[25] different variants of coupled-cluster, and valence bond approaches[26] and the projected Hartree−Fock method.[27] For recent examples, we refer the reader to refs 28−42. By construction, such multireference approaches may correctly capture strong (nondynamic and static) correlation effects.[2,3,6,43] However, to ensure computational tractability, the number of Slater determinants needs to be restricted to handle the factorially growing dimension of the many-particle Hilbert space. This problem is commonly addressed by introducing an active orbital space, possibly composed of different subspaces with method-dependent occupational restrictions. Note that the projected Hartree−Fock method does not require the definition of an active space.[27] The missing weak (dynamic) electron correlation effects, attributed to excitations to the external (i.e., inactive virtual) orbitals, can be added *a posteriori* in a perturbative way.[44−50]

A conceptually different group of approaches that are well-suited for strongly correlated electrons uses two-electron functions, called geminals, to build electron correlation effects into the many-particle wave function.[51−55] In its second-quantized form, a geminal wave function can be written as

$$|\Psi_{\text{geminal}}\rangle = \Psi_1^\dagger \Psi_2^\dagger \ldots \Psi_{N/2}^\dagger |\text{vac}\rangle \tag{1}$$

where the index N is the number of electrons, $|\text{vac}\rangle$ denotes some vacuum state with respect to the creation of geminals and $\Psi_i^\dagger$ is a geminal, that is, a correlated two-electron function. If we confine geminals to be singlet functions, a pair-creation then bears the form

$$\Psi_i^\dagger = \sum_{p,q=1}^{M_i} C_{p,q}^i a_{p\uparrow}^\dagger a_{q\downarrow}^\dagger \tag{2}$$

Special Issue: International Conference on Theoretical and High Performance Computational Chemistry Symposium

Received: February 28, 2014
Revised: April 17, 2014
Published: April 18, 2014

   dx.doi.org/10.1021/jp502127v | J. Phys. Chem. A 2014, 118, 9058−9068

where M_i is the number of one-particle functions (orbitals) used to create geminal i, $C^i_{p,q}$ is a geminal matrix coefficient for subspace M_i, and $a^\dagger_{p\uparrow}$ and $a^\dagger_{q\downarrow}$ are the standard electron creation operators for up- and down-spin electrons ($\uparrow$, $\downarrow$). The geminal matrix coefficient links the geminal wave function with the underlying one-particle basis functions (orbitals). Further, the $C^i_{p,q}$ matrix can be diagonalized for each subspace by an appropriate unitary transformation that brings the geminals into their *natural* form, constructed from the transformed set of natural orbitals,

$$\Psi^\dagger_i = \sum_{p=1}^{M_i} C^i_p \tilde{a}^\dagger_{p\uparrow}\tilde{a}^\dagger_{p\downarrow} \tag{3}$$

Specifically, the geminal matrix structure depends on the geminal wave function ansatz used.[55−58]

Over the past decade, various geminal-based approaches have been introduced in the literature that impose different restrictions on the geminal coefficient matrix $\{C^i_p\}$ (or $\{C^i_{p,q}\}$, respectively) to ease computational cost.[54,55] The most popular approaches are based on the antisymmetric product of strongly orthogonal geminals[51,59−63] (APSG), the antisymmetrized geminal power[52,64] (which is a special case of projected Hartree−Fock−Bogoliubov), or the antisymmetric product of interacting geminals[54−56,65−74] (APIG). In the APSG approach, the subspaces M_i are disjoint, i.e., each geminal is constructed from different orbitals. Thereby, the APSG wave function has a simple and computationally tractable form, but misses a large fraction of the electron correlation energy resulting from the interaction between geminals.[55] The APIG ansatz alleviates this problem by relaxing the strong-orthogonality constraint. However, restoring correlation between all orbital pairs forfeits computational tractability. As a consequence, the application of geminal-based approaches to large and chemically more interesting systems has been limited.

Recently, we have presented new geminal-based wave function ansätze that approximate the APIG wave function, but require significantly less computational cost.[57,58] Specifically, the antisymmetric product of 1-reference orbital geminal (AP1roG)[58,75] provides an alternative parametrization of the doubly occupied configuration interaction (DOCI),[76] but demands only mean-field computational cost in contrast to the factorial scaling of traditional DOCI implementations. The AP1roG wave function ansatz can be rewritten in terms of one-particle functions as a fully general pair-coupled-cluster wave function, that is,

$$|\Psi_{\text{AP1roG}}\rangle = \exp\Big(\sum_{i=1}^{P}\sum_{a=P+1}^{K} C^a_i a^\dagger_a a^\dagger_{\bar{a}} a_{\bar{i}} a_i\Big)|\Phi_0\rangle \tag{4}$$

where $a^\dagger_p$, $a^\dagger_{\bar{p}}$ and a_p, $a_{\bar{p}}$ are the electron creation and annihilation operators, in which p and $\bar{p}$ denote α and β spins, respectively, and $|\Phi_0\rangle$ is some independent-particle wave function (usually the Hartree−Fock determinant). Indices i and a correspond to virtual and occupied orbitals with respect to $|\Phi_0\rangle$, P and K denote the number of electron pairs ($P = N/2$ with N being the total number of electrons) and orbitals, respectively, and $\{C^a_i\}$ are the geminal coefficients (cf., eqs 2 and 3). For AP1roG, the electronic Schrödinger equation can be solved very efficiently by projection onto the set of pair excitations,[58]

$$\langle\Phi_0|\hat{H}|\Psi_{\text{AP1roG}}\rangle = E\langle\Phi_0|\Psi_{\text{AP1roG}}\rangle \tag{5}$$

$$\langle\Phi^{a\bar{a}}_{i\bar{i}}|\hat{H}|\Psi_{\text{AP1roG}}\rangle = E\langle\Phi^{a\bar{a}}_{i\bar{i}}|\Psi_{\text{AP1roG}}\rangle \tag{6}$$

where $\hat{H}$ is some Hamiltonian and $\langle\Phi^{a\bar{a}}_{i\bar{i}}|$ are pair excitations with respect to some reference wave function $\langle\Phi_0|$. We should emphasize that the exponential form of eq 4 guarantees size-extensivity.

The AP1roG approach can be combined with an orbital optimization protocol[77] (abbreviated by the acronym OO-AP1roG) that is analogous to the orbital-optimized coupled cluster approach.[78−80] The (variational) optimization of the one-particle basis functions restores size-consistency, provided that the optimized orbitals are localized,[77] that is, symmetry-broken. In particular, OO-AP1roG poses a mean-field-like approximation to DO-Self-Consistent-Field (DOSCF).[76]

In our second (variational) approach, we have employed the eigenvectors of the reduced Bardeen−Cooper−Schrieffer (BCS) Hamiltonian[81]

$$\hat{H}_{\text{BCS}} = \sum_{i=1}^{N} \varepsilon_i (a^\dagger_{i\uparrow}a_{i\uparrow} + a^\dagger_{i\downarrow}a_{i\downarrow}) - g\sum_{ij} a^\dagger_{i\uparrow}a^\dagger_{i\downarrow}a_{j\downarrow}a_{j\uparrow} \tag{7}$$

as trial wave functions. The system is defined by the set of single-particle energies $\{\varepsilon_i\}$, and the pairing strength g. Eigenvectors of the reduced BCS Hamiltonian have the form of a Bethe ansatz[82] in terms of the geminals

$$\Psi^\dagger_i = \sum_{p=1}^{M} \frac{1}{\lambda_i - \varepsilon_p} a^\dagger_{p\uparrow}a^\dagger_{p\downarrow} \tag{8}$$

Each pair of electrons is labeled with a *rapidity* or *pair energy* λ. With the use of the reduced BCS Hamiltonian on a product of these rank 2 geminals one can readily observe that an eigenvector is obtained provided that the rapidities satisfy Richardson's equations[83,84]

$$\frac{1}{g} + \sum_{p=1}^{M}\frac{1}{\lambda_i - \varepsilon_p} - 2\sum_{j\neq i}\frac{1}{\lambda_i - \lambda_j} = 0, \qquad i = 1, \ldots, N/2. \tag{9}$$

To solve this set of equations numerically we have employed the algorithm proposed by De Baerdemacker et al.,[85] though other algorithms are prevalent.[86−88] Practical expressions for the 1- and 2-reduced density matrices are known.[89] We will refer to this trial wave function as the antisymmetric product of rank 2 geminals (APr2G).[57]

In this work, we assess the accuracy of our recently presented geminal-based approaches (AP1roG and APr2G) in describing the ground-state electronic structure of a test set of diatomic molecules and their spectroscopic constants (bond lengths, potential depths, and harmonic vibrational frequencies). Specifically, we focus on the LiH, Li_2, HF, and C_2 molecules, where accurate theoretical benchmark and experimental spectroscopic data are available. In addition, we investigate the performance of simple perturbative corrections[90] to the OO-AP1roG wave function.

■ COMPUTATIONAL DETAILS

The full configuration interaction (FCI), the DOCI, and the DOSCF energies were obtained using the Molpro2010 software package.[91] The (restricted) second-order Møller−Plesset (MP2) perturbation theory, (restricted) coupled cluster theory with singles, doubles, and perturbative triples (CCSD(T)) and including full triples (CCSDT), as well as the

dx.doi.org/10.1021/jp502127v | J. Phys. Chem. A 2014, 118, 9058−9068

Table 1. Spectroscopic Constants: Bond Distances (R_e), Potential Energy Depths (D_e) and Harmonic Vibrational Frequencies (ω_e) for the $X\ ^1\Sigma^+$ State of the LiH Molecule. Differences with Respect to FCI (in a Given Basis Set) Are Listed in Parentheses

method	basis set	R_e [Å]	D_e [eV]	ω_e [cm^{-1}]
APr2G-A	cc-pVDZ	1.619 (+0.004)	3.569 (+1.314)	1388.7 (+35.9)
AP1roG	cc-pVDZ	1.621 (+0.006)	3.506 (+1.251)	1385.5 (+32.7)
DOCI	cc-pVDZ	1.621 (+0.006)	3.506 (+1.251)	1385.5 (+32.7)
APr2G-B	cc-pVDZ	1.616 (+0.001)	2.250 (−0.005)	1344.6 (−8.2)
OO-AP1roG	cc-pVDZ	1.616 (+0.001)	2.253 (−0.002)	1354.8 (+2.0)
DOSCF	cc-pVDZ	1.616 (+0.001)	2.253 (−0.002)	1354.8 (+2.0)
OO-AP1roG-PTa	cc-pVDZ	1.615 (+0.000)	2.254 (−0.001)	1352.4 (−0.4)
OO-AP1roG-PTb	cc-pVDZ	1.615 (+0.000)	2.254 (−0.001)	1353.1 (+0.3)
DFT/PBE	cc-pVDZ	1.623 (+0.008)	2.895 (+0.640)	1354.7 (+1.9)
MP2	cc-pVDZ	1.612 (−0.003)	3.418 (+1.163)	1379.5 (+26.7)
CCSD(T)	cc-pVDZ	1.614 (−0.001)	2.249 (−0.006)	1352.9 (+0.1)
FCI	cc-pVDZ	1.615	2.255	1352.8
AP1roG	aug-cc-pVDZ	1.595 (+0.011)	4.000 (+1.572)	1456.4 (+22.3)
DOCI	aug-cc-pVDZ	1.595 (+0.011)	4.000 (+1.572)	1456.4 (+22.3)
OO-AP1roG	aug-cc-pVDZ	1.590 (+0.006)	2.413 (−0.015)	1421.4 (−12.7)
DOSCF	aug-cc-pVDZ	1.590 (+0.006)	2.413 (−0.015)	1421.6 (−12.5)
OO-AP1roG-PTa	aug-cc-pVDZ	1.585 (+0.001)	2.425 (−0.003)	1432.1 (−2.0)
OO-AP1roG-PTb	aug-cc-pVDZ	1.586 (+0.002)	2.425 (−0.003)	1437.4 (+3.3)
DFT/PBE	aug-cc-pVDZ	1.617 (+0.033)	2.997 (+0.569)	1347.6 (−86.5)
MP2	aug-cc-pVDZ	1.587 (+0.003)	3.551 (+1.123)	1457.6 (+23.5)
CCSD(T)	aug-cc-pVDZ	1.583 (−0.001)	2.411 (−0.017)	1405.0 (−29.1)
FCI	aug-cc-pVDZ	1.584	2.428	1434.1
AP1roG	aug-cc-pVTZ	1.649 (+0.057)	3.841 (+1.311)	1359.2 (−60.0)
OO-AP1roG	aug-cc-pVTZ	1.600 (+0.008)	2.504 (−0.026)	1395.1 (−24.1)
OO-AP1roG-PTa	aug-cc-pVTZ	1.594 (+0.002)	2.527 (−0.003)	1416.0 (−3.2)
OO-AP1roG-PTb	aug-cc-pVTZ	1.594 (+0.002)	2.525 (−0.005)	1420.5 (+1.3)
DFT/PBE	aug-cc-pVTZ	1.613 (+0.021)	2.698 (+0.168)	1350.9 (−68.3)
MP2	aug-cc-pVTZ	1.589 (−0.003)	3.629 (+1.099)	1441.5 (+22.3)
CCSD(T)	aug-cc-pVTZ	1.592 (−0.000)	2.460 (−0.070)	1406.2 (−13.0)
FCI	aug-cc-pVTZ	1.592	2.530	1419.2
Exp.		1.596[111]	2.515[112]	1405.7[113]

(unrestricted) density functional theory calculations employing the PBE[92] exchange−correlation functional were performed with the NWCHEM6.1 quantum chemistry software.[93−95]

AP1roG/APr2G. The optimization of the (restricted) AP1roG[58] and OO-AP1roG[77] wave functions was done with a local developer version of the HORTON program package.[96] In the OO-AP1roG approach, we used a Newton−Raphson optimizer and a diagonal approximation to the orbital Hessian to obtain the rotated set of orbital expansion coefficients. Furthermore, spatial symmetry was preserved during the orbital optimization procedure; we refer the reader to ref 97 where spectroscopic constants obtained from symmetry-broken solutions are discussed. Two types of second-order perturbative corrections, PTa and PTb, were applied on top of OO-AP1roG, to account for weak (dynamic) electron correlation effects. The main difference between these two approaches is that the former uses the Hartree−Fock determinant and the latter uses the AP1roG wave function as its dual (cf. ref 90 for more details).

The variational APr2G energies were calculated using an "in-house" FORTRAN90 code. Two types of APr2G calculations were performed: using (i) canonical Hartree−Fock orbitals (labeled as APr2G-A) and (ii) OO-AP1roG orbitals (labeled as APr2G-B). The one- and two-electron molecular orbital integrals used for APr2G-A were generated with the DALTON2013 quantum chemistry software.[98] In all calculations mentioned above, we correlated all electrons. (One strength of geminal-based approaches is the removal of the need to specify an active space.)

CASSCF/NEVPT2. The CASSCF and NEVPT2 calculations were carried out using the DALTON2013 software package.[98] We employed a "full-valence" complete active space, which results in eight electrons correlated in five orbitals (CAS(8,5)) for HF and eight electrons correlated in eight orbitals (CAS(8,8)) for C_2. The same active orbitals were used in subsequent NEVPT2 calculations.

Basis Sets. For the LiH and Li_2 molecules, we utilized Dunning's cc-pVDZ (H:(4s1p) → [2s1p], Li:(9s4p1d) → [3s2p1d]), aug-cc-pVDZ (H:(5s2p) → [3s2p], Li:(10s5p2d) → [4s3p2d]) and aug-cc-pVTZ (H:(6s3p2d) → [4s3p2d], Li:(12s6p3d2*f*) → [5s4p3d2f]) basis sets.[99−101] For HF and C_2 the cc-pVDZ (C, F:(9s4p1d) → [3s2p1d]), aug-cc-pVDZ (C, F:(10s5p2d) → [4s3p2d]) and aug-cc-pVTZ (C, F:(11s6p3d2f) → [5s4p3d2f]) basis sets were used.[99−101]

Fitting Procedure. The potential energy curves of diatomic molecules were obtained by varying bond-lengths in a range of 1.2−10.0 Å, 2.2−10.0 Å, 0.7−5.0 Å, and 1.1−3.2 Å for the LiH, Li_2, HF, and C_2 molecules, respectively. The points on the

dx.doi.org/10.1021/jp502127v | J. Phys. Chem. A 2014, 118, 9058−9068

resulting potential energy curve were used for a subsequent generalized Morse function[102] fit to obtain the equilibrium bond lengths (R_e) and potential energy depths (D_e). The harmonic vibrational frequencies (ω_e) were calculated numerically using the five-point finite difference stencil.[103]

RESULTS AND DISCUSSION

LiH. Although LiH is the smallest stable, neutral heteroatomic molecule, it is a particularly interesting system for quantum chemists; its electronic structure changes considerably with the internuclear distance, and the resulting potential energy surface is difficult to describe with traditional (single-reference) methods.[104−107] While the $X^1\Sigma^+$ state of LiH is best represented by the single $1\sigma^2 2\sigma^2$ electronic configuration around the equilibrium structure, its contribution changes when the Li-H bond is stretched. For increasing bond distances, the electronic wave function becomes a mixture of four dominant electronic configurations, $1\sigma^2 2\sigma^2$, $1\sigma^2 3\sigma^2$, and $1\sigma^2 2\sigma^1 3\sigma^1$ (doubly degenerate). Multireference approaches are thus required to correctly model the dissociation limit of the single-bond breaking process in the LiH molecule.[105,107−110]

Table 1 lists all bond distances (R_e), potential energy depths (D_e), and harmonic vibrational frequencies (ω_e) for the $X^1\Sigma^+$ state of LiH determined from different quantum chemistry methods and basis sets. For each set of spectroscopic constants, the difference with respect to the exact result in a given basis set is provided in parentheses.

In general, APr2G and AP1roG result in similar spectroscopic constants, which agree well with the DOCI reference data. While equilibrium bond lengths and harmonic vibrational frequencies are in reasonable agreement with FCI, the potential depth is overestimated by more than 1 eV. Similarly, DFT and MP2 fail to predict accurate dissociation energies.

Orbital optimization within the AP1roG approach alleviates these large discrepancies and reduces the differences in the potential well depth to only 0.005 and 0.002 eV for APr2G-B and OO-AP1roG, respectively. We should note that OO-AP1roG can reproduce DOSCF along the dissociation pathway, and thus both methods yield identical spectroscopic constants. The missing weak (dynamic) electron correlation effects can be easily captured by an *a posteriori* perturbative treatment on top of the OO-AP1roG wave function (cf. Table 1 for OO-AP1roG-PTa and OO-AP1roG-PTb results).

Potential energy surfaces for the dissociation process of LiH using the cc-pVDZ basis set are presented in Figure 1. It is important to stress that the dissociation limit has been shifted to zero a.u. in all approaches and, apart from our DFT/PBE results, all total energies are higher than the FCI reference. In general, OO-AP1roG, OO-AP1roG-PTa/PTb, APr2G-B, DOSCF, and CCSD(T) lie on top of the FCI reference curve for all basis sets studied (see Figures S1 and S2 of the Supporting Information for further details). A systematic improvement in the basis set size (cc-pVDZ → aug-cc-pVDZ → aug-cc-pVTZ) brings the theoretically determined spectroscopic constants very close to experimental data (cf. Table 1). Additional figures (S1 and S2) with potential energy surfaces for larger basis sets can be found in the Supporting Information.

Li_2. Although being the second smallest, just after molecular hydrogen, stable homonuclear molecule, Li_2 has attracted a lot of attention from quantum chemists.[114−116] Specifically, the lithium dimer serves as a convenient test system of theoretical methods and represents the smallest prototype for a theoretical description of long-range potential energy curves in molecular photoassociative spectroscopy of cold alkali atoms.[117]

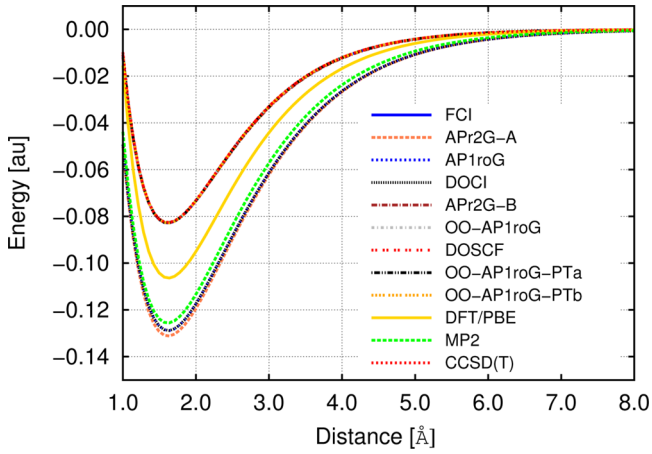

Figure 1. Fitted potential energy surface of the ground state of the LiH molecule obtained from different quantum chemistry methods using the cc-pVDZ basis set. Note that the dissociation limit is shifted to zero for all approaches.

Spectroscopic constants for the $^1\Sigma_g^+$ ground state of Li_2 are collected in Table 2. APr2G-A and AP1roG provide a qualitatively incorrect dissociation limit and overestimate equilibrium bond-lengths. The same is true for DOCI, which gives similar results to AP1roG (see Table 2). We should note that APr2G includes AP1roG as a special case only for four-electron systems.[57]

Optimizing the one-particle basis functions for geminals improves all spectroscopic constants, giving excellent agreement with FCI or CCSD(T)/CCSDT reference data for all basis sets studied (see also Figure 2). Minor differences for larger basis sets are attributed to weak (dynamic) electron correlation effects (see Figures S3 and S4 of the Supporting Information). This type of electron correlation is not directly included in our geminal-based wave function ansätze, but can easily be recovered *a posteriori* in, e.g., OO-AP1roG-PTa and OO-AP1roG-PTb. In particular, spectroscopic constants determined from OO-AP1roG-PTa or OO-AP1roG-PTb are in line with the corresponding CCSD(T) and CCSDT results. Finally, we should emphasize that only OO-AP1roG-PTa and OO-AP1roG-PTb as well as CCSD(T) and CCSDT in combination with a large basis set yield spectroscopic constants that are in agreement with experimental data (cf. Table 2), while DFT and MP2 fail in describing the potential energy curve of Li_2 overestimating equilibrium bond distances and dissociation energies.

HF. The dissociation of hydrogen fluoride represents another toy model for multireference approaches.[8,119] Similar to lithium hydride, the HF molecule is well represented by a single $1\sigma^2 2\sigma^2 3\sigma^2 1\pi^4$ electronic configuration around the equilibrium interatomic distance, while for stretched interatomic bond lengths, two additional electronic configurations, $1\sigma^2 2\sigma^2 1\pi^4 4\sigma^2$ and $1\sigma^2 2\sigma^2 1\pi^4 3\sigma^1 4\sigma^1$, become important.[110,119] The alternating interplay of weak and strong electron correlation effects along the dissociation pathway makes the HF molecule a very difficult test case for single-reference quantum chemistry methods.[110]

All spectroscopic constants for the $X^1\Sigma^+$ state of the HF molecule are listed in Table 3, while the potential energy surfaces are illustrated in Figure 3. We should stress that larger deviations between the OO-AP1roG and DOSCF results arise

dx.doi.org/10.1021/jp502127v | J. Phys. Chem. A 2014, 118, 9058−9068

Table 2. Spectroscopic Constants: Bond Distances (R_e), Potential Energy Depths (D_e) and Harmonic Vibrational Frequencies (ω_e) for the $X\ ^1\Sigma_g^+$ State of the Li_2 Molecule. Differences with Respect to Reference Data (in a Given Basis Set) Are Listed in Parentheses

method	basis set	R_e [Å]	D_e [eV]	ω_e [cm^{-1}]
APr2G-A	cc-pVDZ	2.821 (+0.109)	0.705 (−0.278)	310.3 (−23.9)
AP1roG	cc-pVDZ	2.785 (+0.073)	0.796 (−0.187)	324.3 (−9.9)
DOCI	cc-pVDZ	2.785 (+0.073)	0.796 (−0.187)	324.3 (−9.9)
APr2G-B	cc-pVDZ	2.719 (+0.007)	0.849 (−0.134)	330.8 (−3.4)
OO-AP1roG	cc-pVDZ	2.720 (+0.008)	0.977 (−0.006)	336.7 (+2.5)
DOSCF	cc-pVDZ	2.721 (+0.009)	0.978 (−0.005)	336.6 (+2.4)
OO-AP1roG-PTa	cc-pVDZ	2.711 (−0.001)	0.984 (+0.001)	334.4 (+0.2)
OO-AP1roG-PTb	cc-pVDZ	2.713 (+0.001)	0.982 (−0.001)	334.1 (−0.1)
DFT/PBE	cc-pVDZ	2.743 (+0.031)	1.440 (+0.457)	329.6 (−4.6)
MP2	cc-pVDZ	2.773 (+0.061)	1.415 (+0.432)	329.7 (−4.5)
CCSD(T)	cc-pVDZ	2.712 (−0.000)	0.979 (−0.004)	334.5 (+0.3)
FCI	cc-pVDZ	2.712	0.983	334.2
AP1roG	aug-cc-pVDZ	2.771 (+0.065)	0.669 (−0.327)	338.8 (+7.8)
OO-AP1roG	aug-cc-pVDZ	2.718 (+0.012)	0.987 (−0.009)	334.4 (+3.4)
OO-AP1roG-PTa	aug-cc-pVDZ	2.703 (−0.002)	0.996 (+0.000)	331.0 (+0.0)
OO-AP1roG-PTb	aug-cc-pVDZ	2.703 (−0.002)	0.994 (−0.002)	329.3 (−1.7)
DFT/PBE	aug-cc-pVDZ	2.741 (+0.035)	1.439 (+0.443)	329.9 (−1.1)
MP2	aug-cc-pVDZ	2.764 (+0.058)	1.434 (+0.438)	328.3 (−2.7)
CCSD(T)	aug-cc-pVDZ	2.704 (−0.002)	0.991 (−0.005)	330.6 (−0.4)
FCI	aug-cc-pVDZ	2.706	0.996	331.0
AP1roG	aug-cc-pVTZ	2.784 (+0.123)	0.628 (−0.452)	349.1 (+2.2)
OO-AP1roG	aug-cc-pVTZ	2.690 (+0.029)	1.039 (−0.041)	340.4 (−6.5)
OO-AP1roG-PTa	aug-cc-pVTZ	2.661 (+0.000)	1.086 (+0.006)	344.9 (−2.0)
OO-AP1roG-PTb	aug-cc-pVTZ	2.666 (+0.005)	1.066 (−0.014)	342.7 (−4.2)
DFT/PBE	aug-cc-pVTZ	2.727 (+0.066)	1.451 (+0.371)	331.4 (−15.5)
MP2	aug-cc-pVTZ	2.721 (+0.060)	1.391 (+0.311)	343.2 (−3.7)
CCSD(T)	aug-cc-pVTZ	2.660 (−0.001)	1.054 (−0.026)	247.2 (+0.3)
CCSDT	aug-cc-pVTZ	2.661	1.080	346.9
Exp.		2.673[118]	1.050[118]	351.4[118]

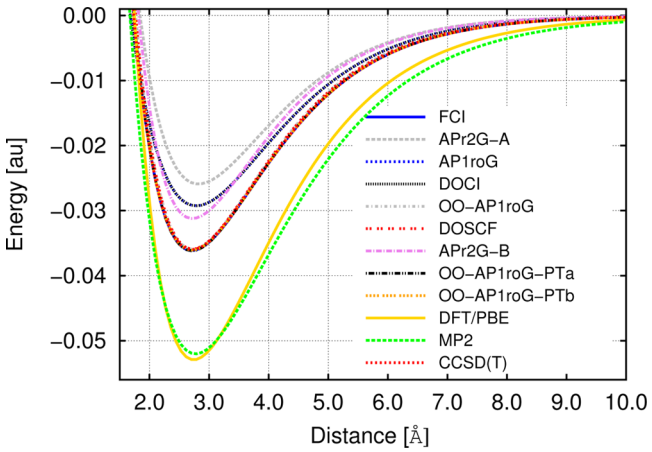

Figure 2. Fitted potential energy surface of the ground state of the Li_2 molecule obtained from different quantum chemistry methods using the cc-pVDZ basis set. Note that the dissociation limit is shifted to zero for all approaches.

out of the optimization complexity in DOSCF calculations. While the latter approach has difficulties in dodging local minima, the OO-AP1roG optimization seems more robust.

Optimization of the one-particle basis function is necessary to obtain a qualitatively correct description of spectroscopic constants, especially potential energy depths, within AP1roG. While OO-AP1roG works well for all the spectroscopic parameters, APr2G-B provides only a qualitatively correct description of bond lengths. Perturbative corrections upon OO-AP1roG, that is, OO-AP1roG-PTa, and OO-AP1roG-PTb, further improve bond distances and potential depths. However, opposite to what we observed for LiH and Li_2, these two flavors of perturbation theory yield qualitatively different results (cf. Figure 3 and Table 3). While, OO-AP1roG-PTa systematically overestimates, OO-AP1roG-PTb systematically underestimates dissociation energies for all basis sets. Specifically, OO-AP1roG-PTb yields bond distances and vibrational frequencies that are closest to MR-CISD results for all basis sets studied (cf. Table 3). Yet, the simple PTa-correction is not able to recover dynamic electron correlation effects in a balanced way along the dissociation pathway if the basis set size increases (cc-pVDZ → aug-cc-pVDZ → aug-cc-pVTZ). This drawback amounts to growing discrepancies in potential depths (cf. Table 3 and Figures S5 and S6 of the Supporting Information).

Nonetheless, OO-AP1roG-PTa and OO-AP1roG-PTb outperform DFT as well as standard multireference approaches like CASSCF and NEVPT2 for all basis sets studied and are in closest agreement with reference theoretical (FCI and MR-CISD) and experimental data.

dx.doi.org/10.1021/jp502127v | J. Phys. Chem. A 2014, 118, 9058−9068

Table 3. Spectroscopic Constants: bond Distance (R_e), Potential Energy Depths (D_e) and Harmonic Vibrational Frequencies (ω_e) for the $X\ ^1\Sigma^+$ State of the HF Molecule. Differences with Respect to Reference Data (in a Given Basis Set) Are Listed in Parentheses

method	basis set	R_e [Å]	D_e [eV]	ω_e [cm^{-1}]
AP1roG	cc-pVDZ	0.893 (−0.027)	6.393 (+0.902)	4586.8 (+451.6)
DOCI	cc-pVDZ	0.893 (−0.027)	6.389 (+0.898)	4523.6 (+388.4)
APr2G-B	cc-pVDZ	0.913 (−0.007)	4.166 (−1.325)	4754.1 (+618.8)
OO-AP1roG	cc-pVDZ	0.916 (−0.004)	4.928 (−0.563)	4050.8 (−84.4)
DOSCF	cc-pVDZ	0.916 (−0.004)	4.927 (−0.564)	4139.0 (+3.8)
OO-AP1roG-PTa	cc-pVDZ	0.923 (+0.003)	5.588 (+0.097)	4064.6 (−70.6)
OO-AP1roG-PTb	cc-pVDZ	0.920 (+0.000)	5.245 (−0.246)	4126.8 (−8.4)
DFT/PBE	cc-pVDZ	0.936 (+0.016)	6.916 (+1.425)	3877.6 (−257.6)
CASSCF	cc-pVDZ	0.922 (+0.002)	4.703 (−0.788)	4030.0 (−105.2)
NEVPT2	cc-pVDZ	0.925 (+0.005)	5.695 (+0.204)	4118.5 (−16.7)
MR-CISD[8]	cc-pVDZ	0.920 (+0.000)	5.434 (−0.057)	4143.6 (+8.4)
FCI	cc-pVDZ	0.920	5.491	4135.2
AP1roG	aug-cc-pVDZ	0.901 (−0.022)	7.721 (+2.008)	4302.0 (+263.2)
DOCI	aug-cc-pVDZ	0.903 (−0.020)	7.659 (+1.900)	4209.6 (+115.8)
OO-AP1roG	aug-cc-pVDZ	0.916 (−0.007)	5.221 (−0.538)	4184.2 (+90.4)
OO-AP1roG-PTa	aug-cc-pVDZ	0.927 (+0.004)	5.953 (+0.194)	4006.8 (−87.0)
OO-AP1roG-PTb	aug-cc-pVDZ	0.923 (+0.000)	5.594 (−0.165)	4082.8 (−11.0)
DOSCF	aug-cc-pVDZ	0.919 (−0.004)	5.143 (−0.616)	4161.8 (+68.0)
DFT/PBE	aug-cc-pVDZ	0.935 (+0.012)	6.972 (+1.213)	3903.6 (−190.2)
CASSCF	aug-cc-pVDZ	0.919 (−0.004)	4.928 (−0.831)	4057.6 (−36.2)
NEVPT2	aug-cc-pVDZ	0.930 (+0.007)	6.043 (+0.284)	4058.5 (−35.3)
MR-CISD[8]	aug-cc-pVDZ	0.923	5.759	4093.8
AP1roG	aug-cc-pVTZ	0.904 (−0.015)	7.543 (+1.606)	4528.0 (+382.0)
OO-AP1roG	aug-cc-pVTZ	0.912 (−0.007)	5.336 (−0.601)	4196.7 (+50.7)
OO-AP1roG-PTa	aug-cc-pVTZ	0.921 (+0.002)	6.181 (+0.244)	4095.0 (−51.0)
OO-AP1roG-PTb	aug-cc-pVTZ	0.919 (+0.000)	5.783 (−0.154)	4159.0 (+13.0)
DFT/PBE	aug-cc-pVTZ	0.933 (+0.014)	7.510 (+1.573)	3942.8 (−203.2)
CASSCF	aug-cc-pVTZ	0.917 (−0.002)	4.993 (−0.944)	4135.6 (−10.4)
NEVPT2	aug-cc-pVTZ	0.927 (+0.008)	6.247 (+0.310)	4179.3 (+33.3)
MR-CISD[8]	aug-cc-pVTZ	0.919	5.937	4146.0
Exp.		0.917[118]	6.119[120]	4138.3[118]

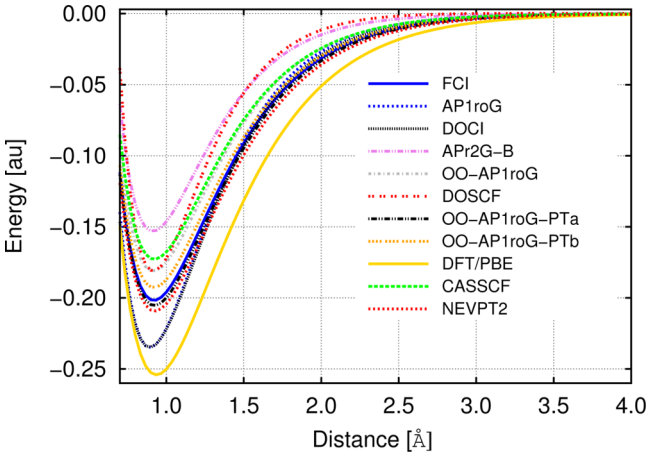

Figure 3. Fitted potential energy surface of the ground state of the HF molecule obtained from different quantum chemistry methods using the cc-pVDZ basis set. Note that the dissociation limit is shifted to zero for all approaches.

C_2. The carbon dimer molecule is an ideal system to test the performance of new electron correlation approaches. This diatomic molecule is known to be poorly described at the single configuration Hartree−Fock level; the ground state electronic structure of C_2 is characterized by two dominant configurations $1\sigma_g^2 1\sigma_u^2 2\sigma_g^2 2\sigma_u^2 1\pi_u^4$ and $1\sigma_g^2 1\sigma_u^2 2\sigma_g^2 1\pi_u^4 3\sigma_g^2$ as well as a number of other configurations arising from low-lying excited states.[7,121−123] The complicated multireference nature of C_2, and the peculiar nature of its chemical bonding, has attracted a lot of attention from theoretical chemists in the past two years.[42,124−127]

Spectroscopic constants of the ground state of the C_2 molecule are summarized in Table 4, while Figure 4 illustrates the optimized potential energy surfaces along the reaction coordinate. We should note that our DOCI, OO-AP1roG-PTa, and OO-AP1roG-PTb results are not shown in Table 4. The DOCI solutions could not be converged due to convergence difficulties and local minima problems; this issue could only partially be resolved for DOSCF calculations. However, we did not make an effort to bypass the local minimum problem in DOSCF calculations due to the unfavorable scaling of the method. Besides, OO-AP1roG-PTa and OO-AP1roG-PTb calculations suffered from intruder-states. As a consequence, we could not obtain reasonable fitting parameters for DOCI, OO-AP1roG-PTa, and OO-AP1roG-PTb.

dx.doi.org/10.1021/jp502127v | J. Phys. Chem. A 2014, 118, 9058−9068

Table 4. Spectroscopic Constants: Bond Distances (R_e), Potential Energy Depths (D_e) and Harmonic Vibrational Frequencies (ω_e) for the $X\ ^1\Sigma_g^+$ State of the C_2 Molecule. Differences with Respect to Reference Data (in a Given Basis Set) Are Listed in Parentheses

method	basis set	R_e [Å]	D_e [eV]	ω_e [cm^{-1}]
AP1roG	cc-pVDZ	1.231 (−0.042)	5.201 (−0.423)	2663.3 (+849.6)
OO-AP1roG	cc-pVDZ	1.240 (−0.033)	5.414 (−0.210)	1930.0 (+116.3)
DOSCF	cc-pVDZ	1.235 (−0.038)	4.981 (−0.643)	2122.7 (+309.0)
CASSCF	cc-pVDZ	1.267 (−0.006)	6.056 (+0.432)	1846.6 (+32.9)
NEVPT2	cc-pVDZ	1.259 (−0.014)	5.893 (+0.269)	1918.3 (+104.6)
DFT/PBE	cc-pVDZ	1.326 (+0.053)	7.261 (+1.637)	718.7 (−1095.0)
DMRG[123]	cc-pVDZ	1.269 (−0.004)	5.628 (+0.004)	1811.4 (−2.3)
FCI[119]	cc-pVDZ	1.273 (+0.000)	not provided	1812.9 (−0.8)
C-MRCI+Q[9]	cc-pVDZ	1.273	5.624	1813.7
AP1roG	aug-cc-pVDZ	1.221 (−0.052)	4.718 (−0.932)	2114.0 (+305.4)
OO-AP1roG	aug-cc-pVDZ	1.240 (−0.033)	5.452 (−0.198)	1938.3 (+129.7)
CASSCF	aug-cc-pVDZ	1.267 (−0.006)	6.047 (+0.397)	1841.2 (+32.6)
NEVPT2	aug-cc-pVDZ	1.259 (−0.014)	5.854 (+0.203)	1924.3 (+115.7)
DFT/PBE	aug-cc-pVDZ	1.193 (−0.080)	7.194 (+1.544)	2257.5 (+448.9)
MR-CISD[7]	aug-cc-pVDZ	1.273	5.650	1808.6
AP1roG	aug-cc-pVTZ	1.199 (−0.053)	4.951 (−1.168)	2862.8 (+1026.8)
OO-AP1roG	aug-cc-pVTZ	1.227 (−0.025)	5.765 (−0.354)	1853.8 (+17.8)
CASSCF	aug-cc-pVTZ	1.255 (+0.003)	6.203 (+0.084)	1841.1 (+5.1)
NEVPT2	aug-cc-pVTZ	1.244 (−0.008)	6.420 (+0.301)	1885.9 (+49.9)
DFT/PBE	aug-cc-pVTZ	1.193 (−0.059)	7.463 (+1.344)	2701.9 (+865.9)
MR-CISD[7]	aug-cc-pVTZ	1.252	6.119	1836.0
Exp.		1.242[118]	6.409 ± 0.022[128]	1854.7[118]

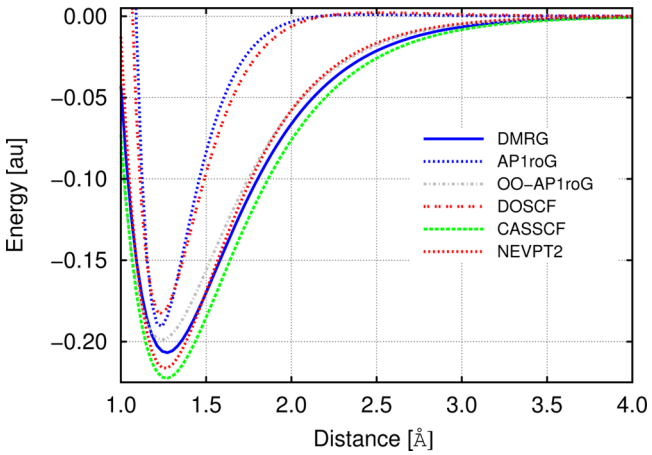

Figure 4. Fitted potential energy surface of the ground state of the C_2 molecule obtained from different quantum chemistry methods using the cc-pVDZ basis set. Note that the dissociation limit is shifted to zero for all approaches.

Since Hartree−Fock provides a poor zeroth-order wave function, APr2G-A and AP1roG give inaccurate spectroscopic constants and qualitatively wrong potential energy surfaces (see Figure 4). This problem can be alleviated by orbital optimization; OO-AP1roG yields spectroscopic constants that are in line with both reference theoretical (DMRG and MR-CISD) and experimental data. Yet, APr2G-B, that is, APr2G with OO-AP1roG-optimized orbitals, converged into an excited state for stretched interatomic distances. Therefore, the APr2G-B spectroscopic constants are not included in our discussion.

Remarkably, the OO-AP1roG outperforms CASSCF and NEVPT2 for D_e and, to some extent, ω_e parameters for all basis sets studied. Larger differences in equilibrium bond lengths originate from the lack of dynamic electron correlation effects that cannot be captured completely by (OO-)AP1roG.

Our DFT/PBE calculations resulted in an unphysical double-minimum potential energy surface caused by spin-contamination in the range of 2.0−3.00 Å of interatomic distance. The fitted dissociation curve is thus not shown in Figure 4. This problem diminishes if larger basis sets (larger than cc-pVDZ) are used (see Figures S7 and S8 of the Supporting Information).

■ CONCLUSIONS

In this work we have investigated the performance of APr2G and AP1roG (using canonical Hartree−Fock orbitals as well as the variationally optimized orbitals of AP1roG). We investigated the spectroscopic constants of LiH, Li_2, HF, and C_2 by comparing the performance of our geminal-based approaches to standard quantum chemistry methods and experimental results. In general, the accuracy of our new geminal-based wave function approaches trends as APr2G-A(canonical HF orbitals) < AP1roG(canonical HF orbitals) < APr2G-B(OO-AP1roG orbitals) < OO-AP1roG. While all four methods yield qualitatively correct bond lengths, a quantitatively accurate description of potential energy depths (D_e) and vibrational frequencies (ω_e) requires optimization of the one-particle basis functions that form the building blocks of geminals. Hence, APr2G-B and OO-AP1roG provide spectroscopic constants (R_e, D_e and ω_e) that are in good agreement with reference theoretical and experimental data.

dx.doi.org/10.1021/jp502127v | J. Phys. Chem. A 2014, 118, 9058−9068

The simple and cheap perturbative corrections PTa and PTb on top of OO-AP1roG improve spectroscopic constants for LiH and Li_2 so that spectroscopic accuracy can be achieved. Yet, for strongly multireference systems, like HF and C_2, the single-reference flavoured PTa and PTb approaches are not appropriate and fail in predicting dissociation energies and vibrational frequencies within spectroscopic accuracy. Different flavors of multireference perturbation theory are currently under investigation in our research group.

In summary, AP1roG and APr2G represent an accurate, cheap, and robust alternative to standard multireference quantum chemistry methods in studying single- and multiple-bond breaking processes in closed-shell systems provided the orbitals are optimized. These new geminal-based methods are size-consistent and size-extensive, and do not require the introduction of active spaces on grounds of computational efficiency. An orbital optimization protocol for APr2G is currently being developed in our laboratory.

■ ASSOCIATED CONTENT

Supporting Information

Potential energy surfaces for the aug-cc-pVDZ and aug-cc-pVTZ basis sets (Figures S1−S8) and potential energy difference plots for the cc-pVDZ basis set (Figures S9−S12). This material is available free of charge via the Internet at http://pubs.acs.org.

■ AUTHOR INFORMATION

Corresponding Author

*E-mail: ayers@mcmaster.ca. Tel.: (905) 525-9140, ext. 24505.

Notes

The authors declare no competing financial interest.

■ ACKNOWLEDGMENTS

We gratefully acknowledge financial support from the Natural Sciences and Engineering Research Council of Canada. K.B. acknowledges the financial support from the Swiss National Science Foundation (P2EZP2 148650). P.A.J. acknowledges funding from a Vanier Canada Graduate Scholarship. T.V. is a postdoctoral researcher funded by the Foundation of Scientific Research, Flanders (FWO). T.V. also received funding from the Research Board of Ghent University (BOF), and BELSPO in the frame of IAP/7/05. The authors acknowledge support for computational resources from SHARCNET, a partner consortium in the Compute Canada national HPC platform. We thank Stijn De Baerdemacker, Dimitri Van Neck, Ward Poelmans, and Patrick Bultinck for many helpful discussions.

■ REFERENCES

(1) Löwdin, P.−O. Quantum Theory of Many-Particle Systems. III. Extension of the Hartree-Fock Scheme To Include Degenerate Systems and Correlation Effects. *Phys. Rev.* **1955**, *97*, 1509−1520.

(2) Bartlett, R. J.; Stanton, J. F. Applications of Post-Hartree−Fock Methods: A Tutorial. *Rev. Comput. Chem.* **1994**, *5*, 65−169.

(3) Bartlett, R. J.; Musiał, M. Coupled-Cluster Theory in Quantum Chemistry. *Rev. Mod. Phys.* **2007**, *79*, 291−350.

(4) Sinanoğlu, O.; Tuan, D. F. Many-Electron Theory of Atoms and Molecules. III. Effect of correlation on orbitals. *J. Chem. Phys.* **1963**, *38*, 1740−1748.

(5) Lee, T. J.; Taylor, P. R. A diagnostic for determining the quality of single-reference electron correlation methods. *Int. J. Quantum Chem.* **1989**, *23*, 199−207.

(6) Boguslawski, K.; Tecmer, P.; Legeza, O.; Reiher, M. Entanglement measures for single- and multireference correlation effects. *J. Phys. Chem. Lett.* **2012**, *3*, 3129−3135.

(7) Peterson, K. A.; Kendall, R. A.; Dunning, T. H. Benchmark calculations with correlated molecular wave functions. III. Configuration interaction calculations on first row homonuclear diatomics. *J. Chem. Phys.* **1993**, *99*, 9790−9805.

(8) Peterson, K. A.; Kendall, R. A.; Dunning, T. H. Benchmark calculations with correlated molecular wave functions. II. Configuration interaction calculations on first row diatomic hydrides. *J. Chem. Phys.* **1993**, *99*, 1930−1944.

(9) Peterson, K. A. Accurate multireference configuration interaction calculations on the lowest $1\Sigma^+$ and 3Π electronic states Of C_2, CN^+, BN, and BO^+. *J. Chem. Phys.* **1995**, *102*, 262−277.

(10) Gagliardi, L.; Roos, B. Quantum Chemical Calculations Show That The Uranium Molecule U_2 Has A Quintuple Bond. *Nature* **2005**, *433*, 848−851.

(11) Reiher, M. A theoretical challenge: Transition-metal compounds. *Chimia* **2009**, *63*, 140−145.

(12) Pierloot, K. Transition metals compounds: Outstanding challenges for multiconfigurational methods. *Int. J. Quantum Chem.* **2011**, *111*, 3291−3301.

(13) Dolg, M.; Cao, X. Relativistic pseudopotentials: Their development and scope of applications. *Chem. Rev.* **2012**, *112*, 403−480.

(14) Gagliardi, L.; Roos, B. O. Multiconfigurational quantum chemical methods for molecular systems containing actinides. *Chem. Soc. Rev.* **2007**, *36*, 893−903.

(15) Morss, L. R.; Edelstein, N. M.; Fuger, J. *The Chemistry of the Actinide and Transactinide Elements*; Springer: Dordrecht, The Netherlands, 2010.

(16) Buenker, R. J.; Peyerimhoff, S. D.; Butscher, W. Applicability of the Multi-Reference Double-Excitation (MRD-CI) Method to the Calculation of Electronic Wavefunctions and Comparison with Related Techniques. *Mol. Phys.* **1978**, *35*, 771−791.

(17) Roos, B.; Taylor, P. R. A Complete Active Space SCF Method-(CASSCF) Using a Density Matrix Formulated Super-CI Approach. *Chem. Phys.* **1980**, *48*, 157−173.

(18) Siegbahn, P. E. M.; Almlöf, J.; Heiberg, A.; Roos, B. O. The Complete Active Space SCF (CASSCF) Method in a Newton−Raphson Formulation with Application to the HNO Molecule. *J. Chem. Phys.* **1981**, *74*, 2384−2396.

(19) Olsen, J.; Roos, B. O.; Jørgensen, P.; Jensen, H. J. A. Determinant Based Configuration Interaction Algorithms for Complete and Restricted Configuration Interaction Spaces. *J. Chem. Phys.* **1988**, *89*, 2185−2192.

(20) White, S. R. Density Matrix Formulation for Quantum Renormalization Groups. *Phys. Rev. Lett.* **1992**, *69*, 2863−2866.

(21) Legeza, O.; Noack, R.; Sólyom, J.; Tincani, L. In *Computational Many-Particle Physics*; Fehske, H., Schneider, R., Weiße, A., Eds.; Lect. Notes Phys.; Springer: Berlin/Heidelberg, 2008; Vol. *739*, pp 653−664.

(22) Marti, K. H.; Reiher, M. The Density Matrix Renormalization Group Algorithm in Quantum Chemistry. *Z. Phys. Chem.* **2010**, *224*, 583−599.

(23) Marti, K. H.; Reiher, M. New Electron Correlation Theories for Transition Metal Chemistry. *Phys. Chem. Chem. Phys.* **2011**, *13*, 6750−6759.

(24) Chan, G. K.-L.; Sharma, S. The Density Matrix Renormalization Group in Quantum Chemistry. *Annu. Rev. Phys. Chem.* **2011**, *62*, 465−481.

(25) Lyakh, D. I.; Musiał, M.; Lotrich, V. F.; Bartlett, J. Multireference Nature of Chemistry: The Coupled-Cluster View. *Chem. Rev.* **2012**, *112*, 182−243.

(26) Cullen, J. Generalized Valence Bond Solutions from a Constrained Coupled Cluster Method. *Chem. Phys.* **1996**, *202*, 217−229.

(27) Jiménez-Hoyos, C. A.; Henderson, T. M.; Tsuchimochi, T.; Scuseria, G. E. Projected Hartree−Fock Theory. *J. Chem. Phys.* **2012**, *136*, 164109.
(28) Marti, K. H.; Malkin Ondík, I.; Moritz, G.; Reiher, M. Density Matrix Renormalization Group Calculations on Relative Energies of Transition Metal Complexes and Clusters. *J. Chem. Phys.* **2008**, *128*, 014104.
(29) Zgid, D.; Nooijen, M. The Density Matrix Renormalization Group Self-Consistent Field Method: Orbital Optimization with the Density Matrix Renormalization Group Method in the Active Space. *J. Chem. Phys.* **2008**, *128*, 144116.
(30) Kurashige, Y.; Yanai, T. High-Performance ab Initio Density Matrix Renormalization Group Method: Applicability to Large-Scale Multireference Problems for Metal Compounds. *J. Chem. Phys.* **2009**, *130*, 234114.
(31) Ma, D.; Li Manni, G.; Gagliardi, L. The Generalized Active Space Concept in Multiconfigurational Self-Consistent Field Methods. *J. Chem. Phys.* **2011**, *135*, 044128.
(32) Boguslawski, K.; Marti, K. H.; Reiher, M. Construction Of CASCI-Type Wave Functions for Very Large Active Spaces. *J. Chem. Phys.* **2011**, *134*, 224101.
(33) Sharma, S.; Chan, G. K.-L. Spin-Adapted Density Matrix Renormalization Group Algorithms for Quantum Chemistry. *J. Chem. Phys.* **2012**, *136*, 124121.
(34) Boguslawski, K.; Marti, K. H.; Legeza, O.; Reiher, M. Accurate *ab Initio* Spin Densities. *J. Chem. Theory Comput.* **2012**, *8*, 1970−1982.
(35) Rodríguez-Guzmán, R.; Schmid, K. W.; Jiménez-Hoyos, C. A.; Scuseria, G. E. Symmetry-Projected Variational Approach for Ground and Excited States of the Two-Dimensional Hubbard Model. *Phys. Rev. B* **2012**, *85*, 245130.
(36) Rodríguez-Guzmán, R.; Jiménez-Hoyos, C. A.; Schutski, R.; Scuseria, G. E. Multireference Symmetry-Projected Variational Approaches for Ground and Excited States of the One-Dimensional Hubbard Model. *Phys. Rev. B* **2013**, *87*, 235129.
(37) Wouters, S.; Limacher, P. A.; Van Neck, D.; Ayers, P. W. Longitudinal Static Optical Properties of Hydrogen Chains: Finite Field Extrapolations of Matrix Product State Calculations. *J. Chem. Phys.* **2012**, *136*, 134110.
(38) Kurashige, Y.; Chan, G. K.-L.; Yanai, T. Entangled Quantum Electronic Wavefunctions of The Mn_4CaO_5 Cluster in Photosystem II. *Nat. Chem.* **2013**, *5*, 660−666.
(39) Li Manni, G.; Ma, D.; Aquilante, F.; Olsen, J.; Gagliardi, L. Split GAS Method for Strong Correlation and the Challenging Case of Cr_2. *J. Chem. Theory Comput.* **2013**, *9*, 3375−3384.
(40) Tecmer, P.; Boguslawski, K.; Legeza, O.; Reiher, M. Unravelling the Quantum-Entanglement Effect of Noble Gas Coordination on the Spin Ground State of CUO. *Phys. Chem. Chem. Phys.* **2014**, *16*, 719−727.
(41) Knecht, S.; Legeza, O.; Reiher, M. Four-Component Density Matrix Renormalization Group. *J. Chem. Phys.* **2014**, *140*, 041101.
(42) Mottet, M.; Tecmer, P.; Boguslawski, K.; Legeza, O.; Reiher, M. Quantum Entanglement in Carbon−Carbon, Carbon−Phosphorus, and Silicon−Silicon Bonds. *Phys. Chem. Chem. Phys.* **2014**, *16*, 8872−8880.
(43) Roos, B. *Radiation Induced Molecular Phenomena in Nucleic Acids*; Springer: Netherlands, 2008; pp 125−156.
(44) Andersson, K.; Malmqvist, P.-A.; Roos, B. O.; Sadlej, A. J.; Woliński, K. Second-Order Perturbation Theory with a CASSCF Reference Function. *J. Phys. Chem.* **1990**, *94*, 5483−5488.
(45) Andersson, K.; Malmqvist, P.-A.; Roos, B. O. Second-Order Perturbation Theory with a Complete Active Space Self-Consistent Field Reference Function. *J. Chem. Phys.* **1992**, *96*, 1218−1226.
(46) Angeli, C.; Cimiraglia, R.; Evangelisti, S.; Leininger, T.; Malrieu, J.-P. Introduction of N-Electron Valence States for Multireference Perturbation Theory. *J. Chem. Phys.* **2001**, *114*, 10252−10264.
(47) Malmqvist, P.-A.; Pierloot, K.; Shahi, A. R. M.; Cramer, C. J.; Gagliardi, L. The Restricted Active Space Followed by Second-Order Perturbation Theory Method: Theory and Application to the Study of CuO_2 and Cu_2O_2 Systems. *J. Chem. Phys.* **2008**, *128*, 204109.
(48) Pulay, P. A Perspective on the CASPT2Method. *Int. J. Quantum Chem.* **2011**, *111*, 3273−3279.
(49) Yanai, T.; Kurashige, Y.; Neuscamman, E.; Chan, G. K.-L. Multireference Quantum Chemistry through a Joint Density Matrix Renormalization Group and Canonical Transformation Theory. *J. Chem. Phys.* **2010**, *132*, 024105.
(50) Kurashige, Y.; Yanai, T. Second-Order Perturbation Theory with a Density Matrix Renormalization Group Self-Consistent Field Reference Function: Theory and application to the study of chromium dimer. *J. Chem. Phys.* **2011**, *135*, 094104.
(51) Hurley, A. C.; Lennard-Jones, J.; Pople, J. A. The Molecular Orbital Theory of Chemical Valency. XVI. A Theory of Paired-Electrons in Polyatomic Molecules. *Proc. R. Soc. London A* **1953**, *220*, 446−455.
(52) Coleman, A. J. Structure of Fermion Density Matrices. II. Antisymmetrized Geminal Powers. *J. Math. Phys.* **1965**, *6*, 1425−1431.
(53) Miller, K. J.; Klaus, R. Electron Correlation and Augmented Separated-Pair Expansion. *J. Chem. Phys.* **1968**, *48*, 3444−3449.
(54) Surján, P. R. *Correlation And Localization*; Springer: Heidelberg, Germany, 1999; pp 63−88.
(55) Surján, P. R.; Szabados, A.; Jeszenszki, P.; Zoboki, T. Strongly Orthogonal Geminals: Size-Extensive and Variational Reference States. *J. Math. Chem.* **2012**, *50*, 534−551.
(56) Silver, D. M. Bilinear Orbital Expansion of Geminal-Product Correlated Wavefunctions. *J. Chem. Phys.* **1970**, *52*, 299−303.
(57) Johnson, P. A.; Ayers, P. W.; Limacher, P. A.; De Baerdemacker, S.; Van Neck, D.; Bultinck, P. A Size-Consistent Approach to Strongly Correlated Systems Using a Generalized Antisymmetrized Product of Nonorthogonal Geminals. *Comput. Chem. Theory* **2013**, *1003*, 101−113.
(58) Limacher, P. A.; Ayers, P. W.; Johnson, P. A.; De Baerdemacker, S.; Van Neck, D.; Bultinck, P. A New Mean-Field Method Suitable for Strongly Correlated Electrons: Computationally Facile Antisymmetric Products of Nonorthogonal Geminals. *J. Chem. Theory Comput.* **2013**, *9*, 1394−1401.
(59) Parr, R. G.; Ellison, F. O.; Lykos, P. G. Generalized Antisymmetrized Product Wave Functions for Atoms and Molecules. *J. Chem. Phys.* **1956**, *24*, 1106−1107.
(60) Parks, J. M.; Parr, R. G. Theory of Separated Electron Pairs. *J. Chem. Phys.* **1958**, *28*, 335−345.
(61) Kutzelnigg, W. Direct Determination of Natural Orbitals and Natural Expansion Coefficients of Many-Electron Wavefunctions. I. Natural Orbitals in the Geminal Product Approximation. *J. Chem. Phys.* **1964**, *40*, 3640−2647.
(62) Kutzelnigg, W. On the Validity of the Electron Pair Approximation for the Beryllium Ground State. *Theoret. Chim. Acta* **1965**, *3*, 241−253.
(63) Rassolov, V. A. A Geminal Model Chemistry. *J. Chem. Phys.* **2002**, *117*, 5978.
(64) Coleman, A. J. The AGP Model for Fermion Systems. *Int. J. Quantum Chem.* **1997**, *63*, 23−30.
(65) Bratoz, S.; Durand, P. Transposition of the Theories Describing Superconducting Systems to Molecular Systems. Method for Biorbitals. *J. Chem. Phys.* **1965**, *43*, 2670−2679.
(66) Silver, D. M. Natural Orbital Expansion of Interacting Geminals. *J. Chem. Phys.* **1969**, *50*, 5108−5116.
(67) Náray-Szabó, G. All-Pair Wavefunction for Many-Electron States with the Highest Multiplicity. *J. Chem. Phys.* **1973**, *58*, 1775−1776.
(68) Náray-Szabó, G. All-Pair Wave Function and Reduced Variational Equation for Electronic Systems. *Int. J. Qunatum Chem.* **1975**, *9*, 9−21.
(69) Surján, P. R. Interaction of Chemical Bonds: Strictly Localized Wave Functions in Orthogonal Basis. *Phys. Rev. A* **1984**, *30*, 43−50.
(70) Surján, P. R. Interaction of Chemical Bonds. II. Ab Initio Theory for Overlap, Delocalization, and Dispersion Interactions. *Phys. Rev. A* **1985**, *32*, 748−755.
(71) Surján, P. R. The Interaction of Chemical Bonds. III. Perturbed Strictly Localized Geminals. *Int. J. Quantum Chem.* **1994**, *52*, 563−574.

(72) Surján, P. R. The Interaction of Chemical Bonds IV. Interbond Charge Transfer by a Coupled-Cluster-Type Formalism. *Int. J. Quantum Chem.* **1995**, *55*, 109−116.
(73) Rosta, E.; Surján, P. R. Interaction of Chemical Bonds. V. Perturbative Corrections to Geminal-Type Wave Functions. *Int. J. Quantum Chem.* **2000**, *80*, 96−104.
(74) Rosta, E.; Surján, P. R. Two-Body Zeroth Order Hamiltonians in Multireference Perturbation Theory: The APSG Reference State. *J. Chem. Phys.* **2002**, *116*, 878−889.
(75) Limacher, P. A.; Kim, T. D.; Ayers, P. W.; Johnson, P. A.; De Baerdemacker, S.; Van Neck, D.; Bultinck, P. The Influence of Orbital Rotation on the Energy of Closed-Shell Wavefunctions. *Mol. Phys.* **2014**, 853−862.
(76) Weinhold, F.; Wilson, E. B. Reduced Density Matrices of Atoms and Molecules. I. The 2 Matrix of Double-Occupancy, Configuration-Interaction Wavefunctions for Singlet States. *J. Chem. Phys.* **1967**, *46*, 2752−2758.
(77) Boguslawski, K.; Tecmer, P.; Ayers, P. W.; Bultinck, P.; De Baerdemacker, S.; Van Neck, D. *Towards An Efficient Description Of Strongly Correlated Electrons*. 2014, *arXiv:1401.8019*.
(78) Helgaker, T.; Jørgensen, P.; Olsen, J. *Molecular Electronic-Structure Theory*; Wiley: Chichester, UK, 2000.
(79) Scuseria, G. E.; Schaefer, H. F., III The Optimization of Molecular Orbitals for Coupled Cluster Wavefunctions. *Chem. Phys. Lett.* **1987**, *142*, 354−358.
(80) Bozkaya, U.; Turney, J. M.; Yamaguchi, Y.; Schaefer, H. F.; Sherrill, C. D. Quadratically Convergent Algorithm for Orbital Optimization in the Orbital-Optimized Coupled-Cluster Doubles Method and in Orbital-Optimized Second-Order Möller−Plesset Perturbation Theory. *J. Chem. Phys.* **2011**, *135*, 104103.
(81) Bardeen, J.; Cooper, L. N.; Schrieffer, R. Theory of Superconductivity. *Phys. Rev.* **1957**, *108*, 1175−1204.
(82) Bethe, H. Eigenwerte und Eigenfunktionen der Linearen Atomkette. *Z. Phys.* **1931**, *71*, 205−226.
(83) Richardson, R. W. A Restricted Class of Exact Eigenstates of The Pairing-Force Hamiltonian. *Phys. Lett.* **1963**, *3*, 277−279.
(84) Richardson, R. W.; Sherman, N. Exact Eigenstates of The Pairing-Force Hamiltonian. *Nucl. Phys.* **1964**, *52*, 221−238.
(85) De Baerdemacker, S. Richardson-Gaudin Integrability in the Contraction Limit of the Quasispin. *Phys. Rev. C* **2012**, *86*, 044332.
(86) Rombouts, S.; Van Neck, D.; Dukelsky, J. Solving the Richardson Equations for Fermions. *Phys. Rev. C* **2004**, *69*, 061303.
(87) Dominguez, F.; Esebbag, C.; Dukelsky, J. Solving the Richardson Equations Close to the Critical Points. *J. Phys. A: Math. Gen.* **2006**, *39*, 11349−11360.
(88) El Araby, O.; Gritsev, V.; Faribault, A. Bethe Ansatz and Ordinary Differential Equation Correspondence for Degenerate Gaudin Models. *Phys. Rev. B* **2012**, *85*, 115130.
(89) Faribault, A.; Calabrese, P.; Caux, J.-S. Exact Mesoscopic Correlation Functions of the Richardson Pairing Model. *Phys. Rev. B* **2008**, *77*, 064503.
(90) Limacher, P.; Ayers, P.; Johnson, P.; De Baerdemacker, S.; Van Neck, D.; Bultinck, P. Simple and Inexpensive Perturbative Correction Schemes for Antisymmetric Products of Nonorthogonal Geminals. *Phys. Chem. Chem. Phys.* **2014**, *16*, 5061−5065.
(91) Werner, H.-J.; Knowles, P. J.; Lindh, R.; Manby, F. R.; M. Schütz, P. C.; Korona, T.; Mitrushenkov, A.; Rauhut, G.; Adler, T. B.; Amosand, R. D.; et al. *MOLPRO, A Package of Ab Initio Programs*, version 2010.1; Cardiff University: Cardiff, United Kingdom, 2009; http://www.molpro.net.
(92) Perdew, J. P.; Burke, K.; Ernzerhof, M. Generalized Gradient Approximation Made Simple. *Phys. Rev. Lett.* **1996**, *77*, 3865.
(93) Valiev, M.; Bylaska, E.; Govind, N.; Kowalski, K.; Straatsma, T.; Dam, H. V.; Wang, D.; Nieplocha, J.; Apra, E.; Windus, T.; De Jong, W. NWChem: A Comprehensive and Scalable Open-Source Solution for Large Scale Molecular Simulations. *Comput. Phys. Commun.* **2010**, *181*, 1477−1489.
(94) Dam, H. V.; De Jong, W. A.; Bylaska, E.; Govind, N.; Kowalski, K.; Straatsma, T.; Valiev, M. NWChem: Scalable Parallel Computational Chemistry. *Rev. Comput. Mol. Sci.* **2011**, *1*, 888−894.
(95) NWChem, version 6.1. http://www.nwchem-sw.org (accessed on March 1, 2014).
(96) Horton, developer version 1.2, written by T. Verstraelen, S. Vandenrbande, M. Chan, F. H. Zadeh, C. Gonzalez, K. Boguslawski, P. Tecmer, P. A. Limacher, A. Malek, Ghent (Belgium) and Hamilton (Canada), 2013. http://theochem.github.com/horton/ (accessed April 10, 2014).
(97) Boguslawski, K.; Tecmer, P.; Limacher, P. A.; Johnson, P. A.; Ayers, P. W.; Bultinck, P.; De Baerdemacker, S.; Van Neck, D. Projected Seniority-Two Orbital Optimization of The Antisymmetric Product of One-Reference Orbital Geminal. *preprint* **2014**, *arXiv:1404.1426*.
(98) Aidas, K.; Angeli, C.; Bak, K. L.; Bakken, V.; Bast, R.; Boman, L.; Christiansen, O.; Cimiraglia, R.; Coriani, S.; Dahle, P.; et al. The Dalton Quantum Chemistry Program System. *WIREs Comput. Mol. Sci.* **2013**, *4*, 269−284.
(99) Dunning, T. H. Gaussian Basis Sets for Use in Correlated Molecular Calculations. I. The Atoms Boron through Neon and Hydrogen. *J. Chem. Phys.* **1989**, *90*, 1007−1023.
(100) Feller, D. The Role of Databases in Support of Computational Chemistry Calculations. *J. Comput. Chem.* **1996**, *17*, 1571−1586.
(101) Didier, K.; Elsethagen, B.; T. Sun, L. G.; Chase, V.; Li, J.; Windus, T. L. Basis Set Exchange: A Community Database For Computational Sciences. *J. Chem. Inf. Model.* **2007**, *47*, 1045−1052.
(102) Coxon, J. A. The Radial Hamiltonian Operator For LiH $X^1\Sigma^+$. *J. Mol. Spectrosc.* **1992**, *282*, 274−282.
(103) Abramowitz, M.; Stegun, I. A. *Handbook of Mathematical Functions with Formulas, Graphs, and Mathematical Tables*; Dover: New York, 1970.
(104) Ahlrichs, R.; Kutzelnigg, W. Direct Calculation of Approximate Natural Orbitals and Natural Expansion Coefficients of Atomic and Molecular Electronic Wavefunctions. II. Decoupling of the Pair Equations and Calculation of the Pair Correlation Energies for the Be and LiH Ground States. *J. Chem. Phys.* **1968**, *48*, 1819−1832.
(105) Docken, K. K.; Hinze, J. LiH Potential Curves and Wavefunctions For X $^1\Sigma^+$, A $^1\Sigma^+$, B $^1\Pi^3$, A $^3\Sigma^+$ and B $^3\Pi$. *J. Chem. Phys.* **1972**, *57*, 4928−4936.
(106) Li, X.; Paldus, J. An Accurate Determination of Rovibrational Spectra Using the Externally Corrected Coupled-Cluster Approaches: LiH Ground State. *J. Chem. Phys.* **2003**, *118*, 2470−2481.
(107) Li, X.; Paldus, J. The General Model Space State Universal Coupled Cluster Method Exemplified by the LiH Molecule. *J. Chem. Phys.* **2003**, *119*, 5346−5357.
(108) Lee, B. K.; Stout, J. M.; Dykstra, C. E. Ab Initio Calculations of Lithium Hydride. *J. Mol. Struc. (Theochem)* **1997**, *400*, 57−68.
(109) Gadéa, F. X.; Leininger, T. Accurate Ab Initio Calculations for LiH and Its Ions, LiH^+ and LiH^-. *Theor. Chem. Acc.* **2006**, *116*, 566−575.
(110) Das, S.; Mukherjee, D.; Kállay, M. Full Implementation and Benchmark Studies Of Mukherjee's State-Specific Multireference Coupled-Cluster Ansatz. *J. Chem. Phys.* **2010**, *132*, 074103.
(111) Rothstein, E. Molecular Constants of Lithium Hydrides by the Molecular-Beam Electric Resonance Method. *J. Chem. Phys.* **1969**, *50*, 1899−1900.
(112) Velasco, R. Ultraviolet Spectra of LiH and LiD. *Can. J. Phys.* **1957**, *35*, 1204−1214.
(113) Huber, K. P.; Herzberg, G. *Molecular Spectra And Molecular Structure, Vol. IV, Constants Of Diatomic Molecules*; Van Nostrand: New York, 1979.
(114) Scuseria, G. E.; Hamilton, T. P.; Schaefer, H. F. An Assessment for the Full Coupled Cluster Method Including All Single, Double, and Triple Excitations: The Diatomic Molecules LiH, Li_2, BH, LiF, C_2, BeO, CN^+, BF, NO^+, and F_2. *J. Chem. Phys.* **1990**, *92*, 568−573.
(115) Chung, H.-K.; Kirby, K.; Babb, J. F. Theoretical Study of the Absorption Spectra of the Lithium Dimer. *Phys. Rev. A* **1999**, 2002−2008.

(116) Jasik, P.; Sienkiewicz, J. Calculation Of Adiabatic Potentials Of Li_2. *Chem. Phys.* **2006**, *323*, 563−573.
(117) Fioretti, A.; Comparat, D.; Crubellier, A.; Dulieu, O.; Masnou-Seeuws, F.; Pillet, P. Formation of Cold Cs_2 Molecules through Photoassociation. *Phys. Rev. Lett.* **1998**, *80*, 4402−4405.
(118) National Institute of Standards and Technology data base, http://www.nist.gov/chemistry (accessed on March 13, 2014).
(119) Evangelista, F. A. Alternative Single-Reference Coupled Cluster Approaches for Multireference Problems: The Simpler, the Better. *J. Chem. Phys.* **2011**, *134*, 224102.
(120) Zemke, T.; Stwalley, W. C.; Coxon, J. A.; Hajigeorgion, P. G. Improved Potential Energy Curves and Dissociation Energies for HF, DF and TF. *Chem. Phys. Lett.* **1991**, *177*, 412−418.
(121) Abrams, M. L.; Sherrill, C. D. Full Configuration Interaction Potential Energy Curves for the X $^1\Sigma_g^+$, B $^1\Delta_g$, and C $^1\Sigma_g^+$ states of C_2: A Challenge for Approximate Methods. *J. Chem. Phys.* **2004**, *121*, 9211−9211.
(122) Jiménez-Hoyos, C. A.; Rodríguez-Guzmán, R.; Scuseria, G. E. Excited Electronic States from a Variational Approach Based on Symmetry-Projected Hartree-Fock Configurations. *J. Chem. Phys.* **2013**, *139*, 224110.
(123) Wouters, S.; Poelmans, W.; Ayers, P. W.; Neck, D. V. CheMPS2: A Free Open-Source Spin-Adapted Implementation of the Density Matrix Renormalization Group for ab Initio Quantum Chemistry. *Comput. Phys. Commun.* **2014**, *185*, 1501−1514, DOI: 10.1016/j.cpc.2014.01.019.
(124) Shaik, S.; Danovich, D.; Wu, W.; Su, P.; Rzepa, H. S.; Hiberty, P. C. Quadruple Bonding in C_2 and Analogous Eight-Valence Electron Species. *Nat. Chem.* **2012**, *4*, 195−200.
(125) Matxain, J. M.; Ruipérez, F.; Infante, I.; Lopez, X.; Ugalde, J. M.; Merino, G.; Piris, M. Chemical Bonding in Carbon Dimer Isovalent Series from the Natural Orbital Functional Theory Perspective. *J. Chem. Phys.* **2013**, *138*, 151102.
(126) Ramos-Cordoba, E.; Salvador, P.; Reiher, M. Local Spin Analysis and Chemical Bonding. *Chem.—Eur. J.* **2013**, *19*, 15267−15275.
(127) Xu, L. T.; Dunning, T. H. Insights into the Perplexing Nature of the Bonding in C_2 from Generalized Valence Bond Calculations. *J. Chem. Theory Comput.* **2014**, *10*, 195−201.
(128) Urdahl, R. S.; Bao, Y.; Jackson, W. M. An Experimental Determination of the Heat of Formation of C_2 and the C-H Bond-Dissociation Energy in C_2H^-. *Chem. Phys. Lett.* **1991**, *178*, 425−428.